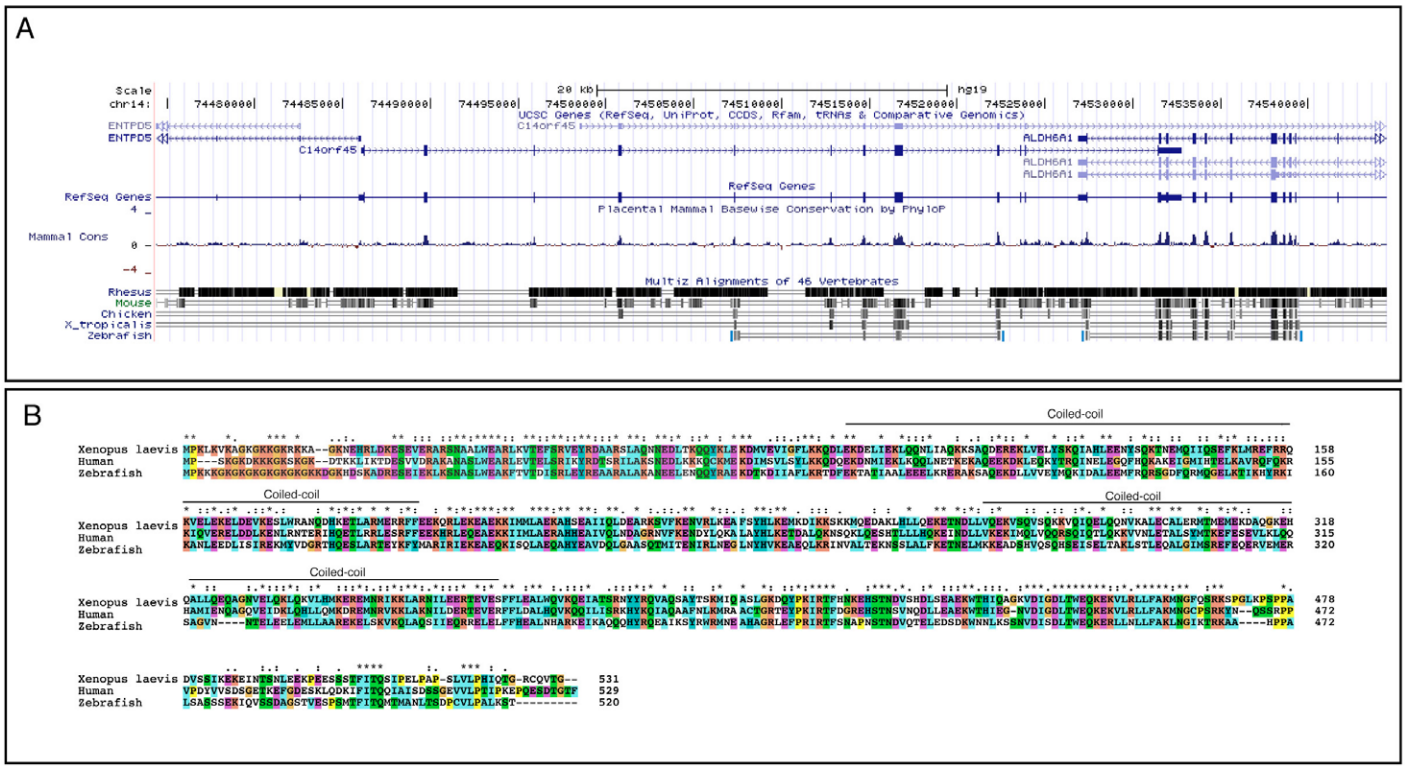

Fig. S1. *bbof1* is a conserved vertebrate gene. (**A**) A screen shot of the UCSC genome browser showing the region of synteny on human chromosome 14 where *BBOF1* (*C14ORF45*) is found, bracketed by the gene encoding NTPDase5 on one side, and the gene encoding aldehyde dehydrogenase on the other. (**B**) Alignment of the bbof1 protein in *Xenopus laevis* with homologs from human and zebrafish. The two regions containing coiled-coil domains are marked with a line, and conserved amino acid residues are marked with an asterisk.

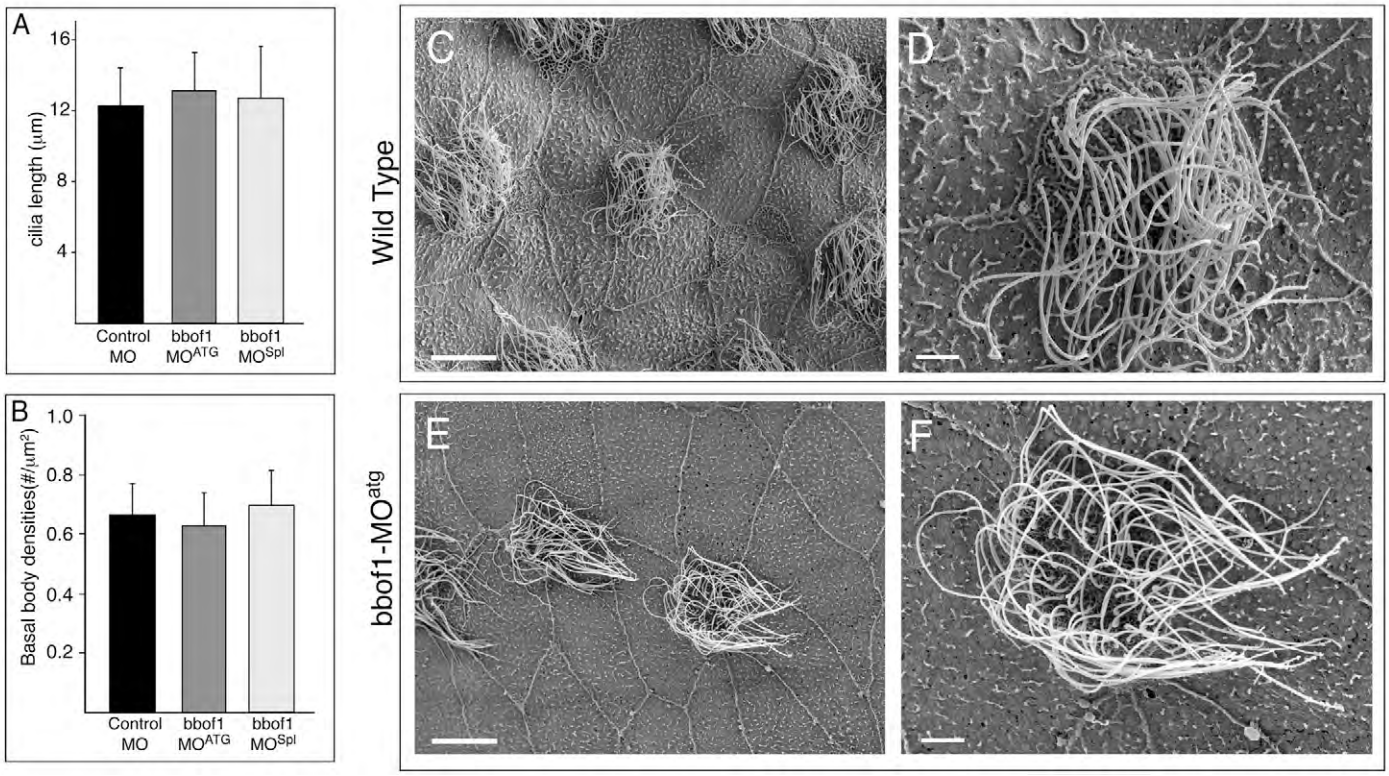

Fig. S2. *bbof1* morphants form normal-appearing MCCs. (**A**,**B**) *Xenopus* embryos were injected at the two-cell stage with a control, bbof1-MO^{atg} or bbof1-MO^{spl} morpholino, followed in some cases by RNAs encoding hyls1-GFP and mRFP to label basal bodies and cell boundaries, respectively. At stage 28, embryos were fixed, stained with an acetylated tubulin antibody to label cilia and imaged by confocal microscopy. Cilia length (A) and basal body density (B) were measured by scoring three to five embryos, collecting data for six to eight cells from each embryo. Error bars indicate s.d. (**C**-**F**) Representative scanning electron micrographs of MCCs in wild type (C,D) and bbof1-MO^{atg} morphants (E,F). Scale bars:10 μm in C and E; 2 μm in D and F.

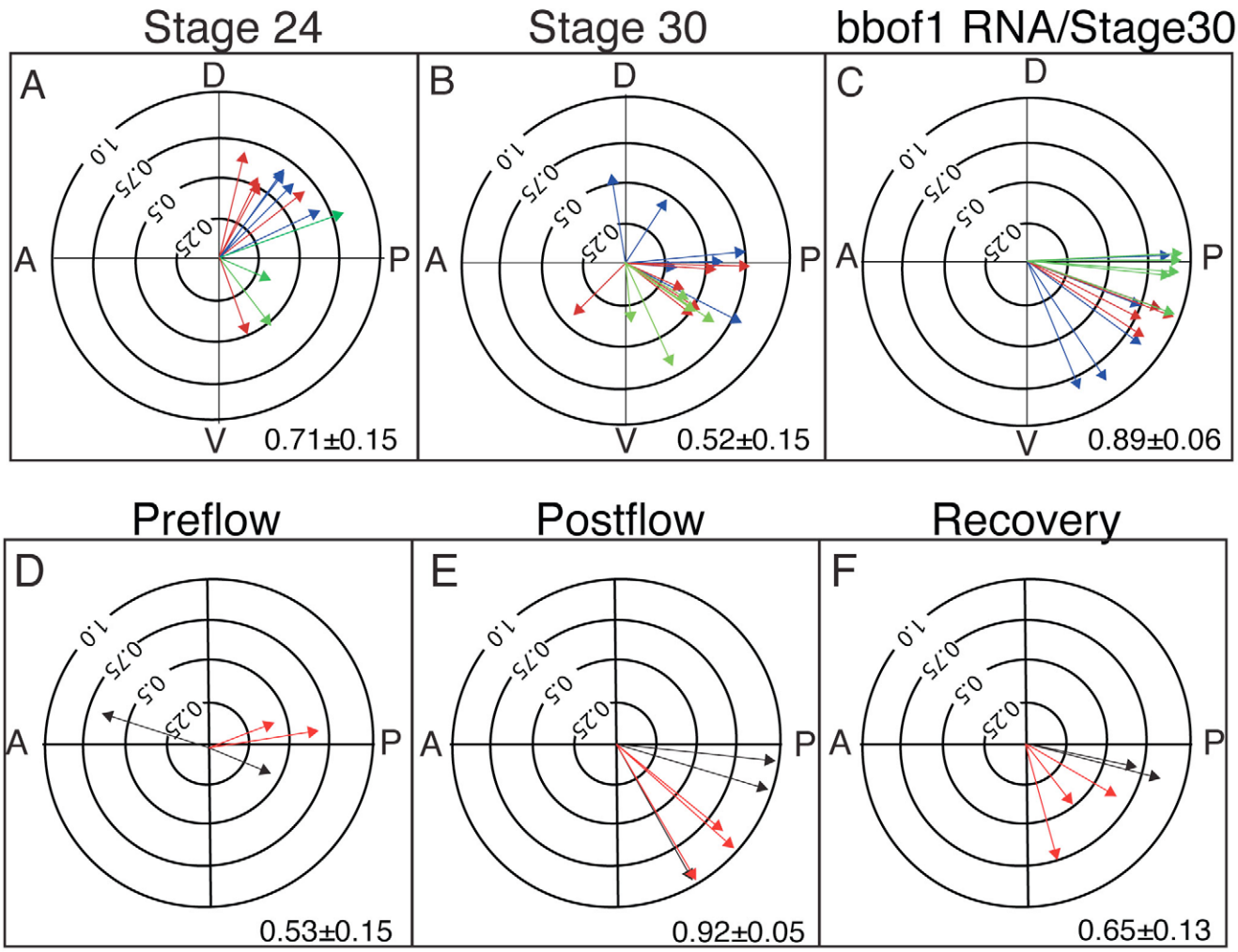

Fig. S3. Cilia orientation in bbof1-MO^{spl} morphants. (**A-C**) Polar plots summarize cilia orientation in bbof1-MO^{spl} morphants, as measured at stage 24 (A), stage 30 (B) or at stage 30 after rescue by injecting a full-length bbof1 RNA (C). This analysis was carried out in parallel with the data shown in the main text Fig. 2D-F and summarized in polar plots as described in the legend to Fig. 2. Each arrow represents data for a single MCC, and arrow color represents MCCs taken from the same embryo. Value in each panel equals the average arrow radius±s.d. for a given condition. (**D-F**) Embryos were injected with the bbof1-MO^{spl} morpholino along with RNA encoding centrin-RFP and clamp-GFP. Ventral explants were treated with an external flow and analyzed as outlined in Fig. 3A in the main text. Shown are polar plots as described in the legend to Fig. 2, summarizing cilia orientation in MCCs before flow treatment (D), 0.5 hours after flow treatment (E) or 5 hours after flow treatment (F). Value in each panel equals the average arrow radius±s.d..

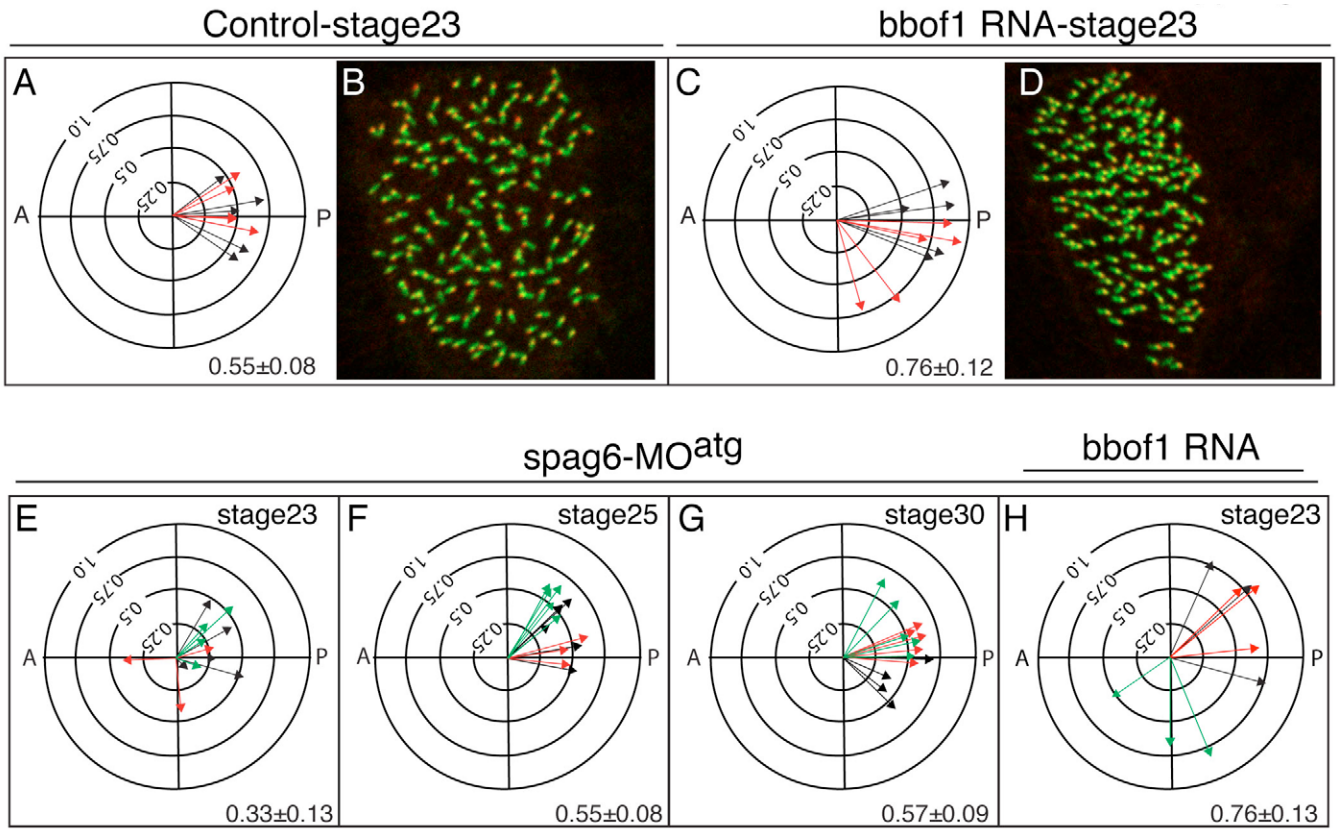

Fig. S4. *bbof1* misexpression promotes premature basal body alignment. (**A-D**) Embryos were injected with RNAs encoding centrin4-RFP and tsga10-GFP, along with RNA encoding a full-length, myc-tagged form of bbof1 (C,D). At stage 23, embryos were fixed, and ciliated cells imaged as shown in B and D, and scored for ciliated cell orientation shown in polar plots (A,C), as described in the legend to Fig. 2. Value in each panel equals the average arrow radius±s.d. (**E-H**) Embryos were injected with a previously described morpholino, spag6-MO^{atg}, which blocks cilia motility (Mitchell et al., 2007), followed by RNA encoding centrin4-RFP and clamp-GFP (E-H) alone, or with RNA encoding a full-length myc-tagged form of bbof1 (H). Embryos were fixed at the indicated stage and scored for ciliated cell orientation, as described in the legend to Fig. 2. Value in each panel equals the average arrow radius±s.d.

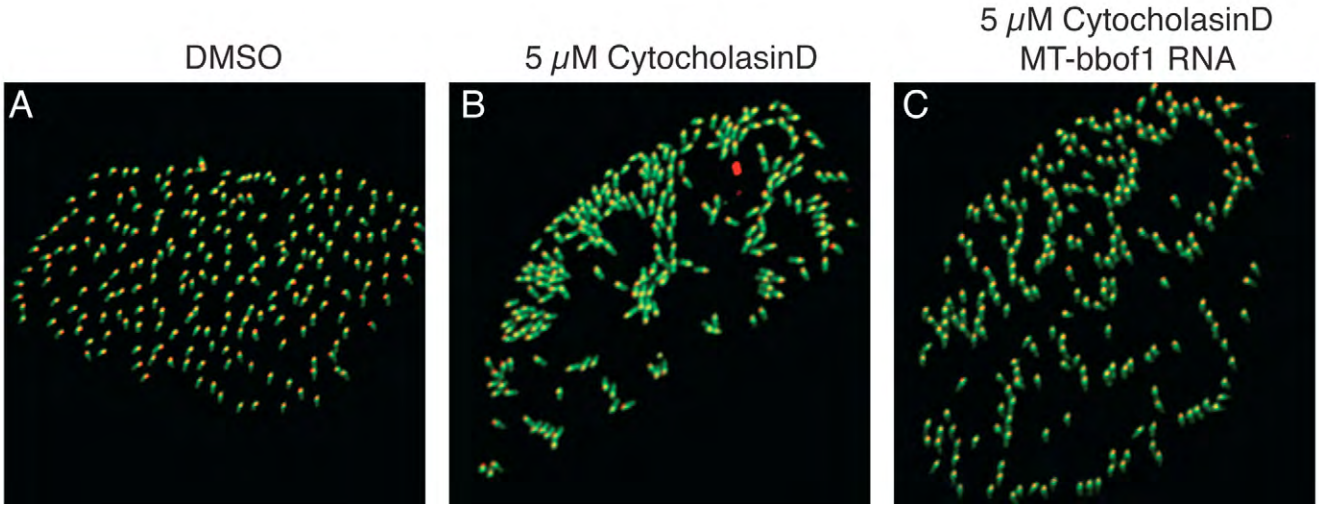

Fig. S5. *bbof1* misexpression fails to rescue the basal body distribution phenotype in embryos treated with cytochalasin D. Embryos were injected with RNAs encoding centrin4-RFP and tsga10-GFP (A-C), along with RNA encoding a full-length, myc-tagged form of bbof1 (C), and then incubated in 5 μM cytochalasin D beginning at stage 23. At stage 30, embryos were fixed and ciliated cells imaged by confocal microscopy. Cytochalasin D treatment causes a clumping phenotype (B) as previously described, as well as a disorientation defect (see Fig. 5). Misexpression of bbof1 partially rescues the latter but does not appear to affect the former phenotype (C).

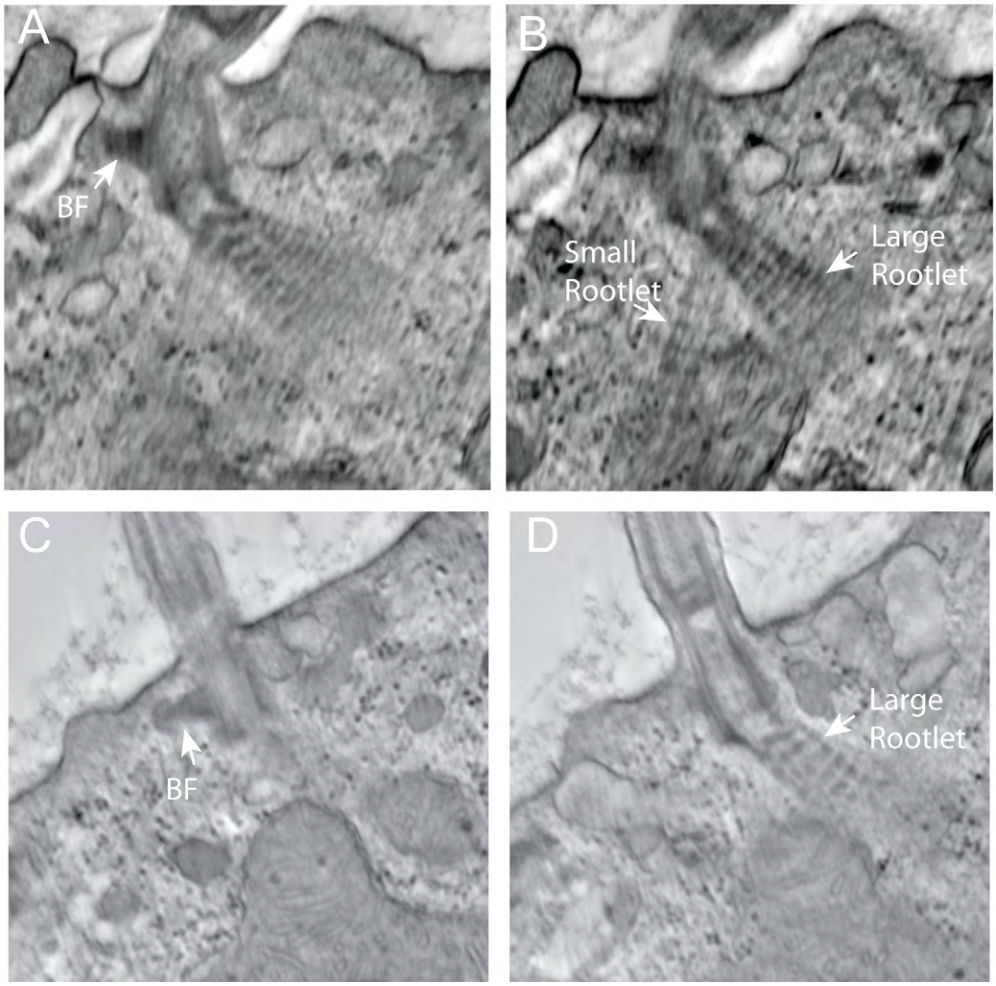

Fig. S6. Ultrastructure of *bbof1* mutant basal bodies. (**A-D**) Slices at the level of the basal foot (A,C) and a large rootlet (B,D) from a wild type (A,B) and bbof1-MO^{spl} morphant (C,D). In wild-type cilia, the rootlet includes a large component, as well as a smaller structure that projects orthogonally deep into the cytoplasm (small rootlet). The small rootlets appear largely absent from the *bbof1* morphant basal bodies (supplementary material Table S1).

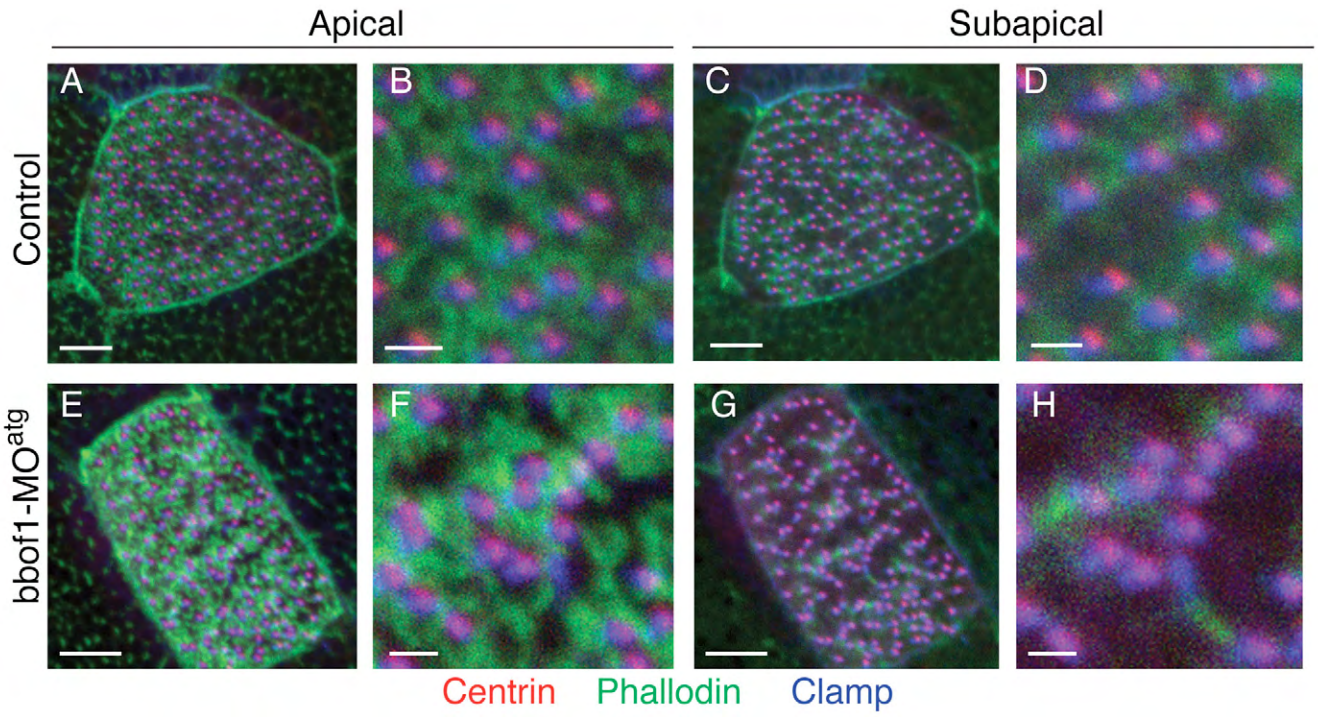

Fig. S7. Phalloidin staining of *bbof1* morphants. Embryos were injected at the two-cell stage with a control (A-D) or bbof1-MO^{atg} morpholino (E-H) followed by RNA encoding centrin4-RFP and clamp-GFP. At stage 30, the embryos were fixed, stained with phalloidin-647 (Werner et al., 2011) and imaged using a Zeiss LSM710 confocal microscope and 63× objective. Shown are representative images of MCCs along with high-magnification images at the level of the apical surface (A-B,E-F) or at the level just below the basal bodies (C-D,G-H, subapical). The phalloidin signal is pseudocolored in green, whereas the clamp-gfp signal is in blue. Scale bars: 5 μm in A,C,E,G; 1 μm in B,D,F,H.

Movie 1. A tomography tilt series produced by imaging a 300 nm section of a wild-type embryo at stage 28 through –60° to 60° in 1° increments, and reconstructed using 25 iterations of the Ordered-Subset Simultaneous Algebraic Reconstruction Technique.

Movie 2. A tomography tilt series similar to the one described for Movie 1, but acquired from a bbof1 morphant embryo.